

A Quantitative Assessment of PET Brain Image Reconstruction using MAP and Neural Network based Segmentation of CG Algorithm

T.Arunprasath¹, M.Pallikonda Rajasekaran² and S.Kannan³

¹ Department of Instrumentation and Control Engineering, Kalasalingam University, Krishnankoil, Virudhunagar DT (TN), 626126. India
arun.aklu@gmail.com

² Department of Electronics and Communication Engineering, Kalasalingam University, Krishnankoil, Virudhunagar DT (TN), 626126. India
mpuja80@gmail.com

³ Department of Electrical and Electronics Engineering, Kalasalingam University, Krishnankoil, Virudhunagar DT (TN), 626126. India
kannaneeps@gmail.com

Abstract: This paper addresses a comparative analysis of PET Brain image reconstruction based on iterative and weighted least-square (WLS) algorithms. In previous years, the analytical approach was used to reconstruct the Positron Emission Tomography (PET). This approach requires a minimization of a convex cost function and accompanied by many problems related to the computational complexity. The poles apart iteration methods are Conjugate Gradient (CG), Coordinate Descent (CD) and Image Space Reconstruction Algorithm (ISRA). It has many advantages compared to conventional approach. The functional protocol used here is neural network based segmentation of PET brain image using CG method to improve the CG algorithm. In this step of process, the image was segmented using Neural Network and reconstructed with CG algorithm. This statistical fashion can provide better and high PSNR along with lowest noise in the PET Brain image. An assortment of image quality parameters is considered to analyze the PET brain image in this algorithm. The PET brain image is constructed and simulated in MATLAB /Simulink package.

Keywords: PET Brain image, CG, Convergence, Iterative algorithm, Image reconstruction, Neural Network

I. Introduction

Medical imaging produces 2- or 3-dimensional images of the internal aspect of the body invasively and noninvasively. It provides the solution of mathematical inverse problems in this restricted sense. Some medical imaging modalities do not penetrate our skin of the body physically. But on the electromagnetic and radiation level, these modalities are quite invasive. From the sky-scraping energy photons in X-Ray Computed Tomography [1,3] to the 2+ Tesla coils of an MRI machine, these modalities change the physical and chemical environment of the body in order to obtain the statistics. But

these techniques are not sufficient to scrutinize the diseases.

Image reconstruction has many applications in various medical fields notably on oncology, neurology, and cardiology. It is classified as 1) positron Emission Tomography 2) Single Photon Emission Computed Tomography. SPECT and PET are used in the Gamma cameras to detect regions of biologic activity that may be associated with disease. Early PET scanners had only a single ring of detectors [4]; hence the acquisition of data and subsequent reconstruction was restricted to a single transverse plane. More recent scanners now include numerous rings, essentially forming a roll of detectors. There are two proposal to reconstructing data from such a scanner: 1) Treat each ring as a split entity, the only chance happening within a ring are perceived the existence, the picture from each ring can then be reconstructed individually, or 2) The coincidences to be perceived the existence between rings as well as within rings, then reconstruct the complete volume together in three dimension.

In nuclear medicine positron emission tomography (PET) camera rotates around the patient, captivating films of radioisotope distribution within the patient from different angles. These films acquired from the camera are called projections. The procedure to put the projections together to obtain a patient's image is called image reconstruction [23]. A single-ring PET camera has been modelled with 128 scintillation crystals on the ring, a detector width of 7.36mm and a field of view (FOV) of 200mm×200mm. The detector ring radius is 150mm. The total number of detector pairs in coincidence is 8128. Several image sizes have been used: 64×64 (pixel size = 3.12 mm), 128×128 (pixel size = 1.56 mm), 256×256 (pixel size = 0.78mm).

Image reconstruction using statistical methods can provide more accurate system prototype, statistical prototype, and

physical constraints than filtered back projection method [6,18]. Nearly all arithmetical methods for image reconstruction require minimizing an objective function related to the measurement information's. For pragmatic image sizes, direct reduction methods are computationally obdurate, thus recursive methods are required. For intention functions that are quadratic, or at least bowed and close by quadratic, conjugate-gradient (CG) algorithms are appealing for reasons of convergence rate. Conjugate-gradient (CG) algorithms is an efficient method that makes good use of diminutive data sets. It also shares the capacity to provide unusual types of easily interpretable statistical intervals for estimation, guess, calibration and optimization.

In this project, we have chosen Positron Emission Tomography to reconstruct the PET brain image. Because it has more number of detected photons compared to SPECT [14]. Positron Emission Tomography (PET) is used to show at how our body uses substances such as glucose, ammonia, water and oxygen. It clearly describes how these molecules move through our body, and where they are being used. By following of trail how our body utilizes glucose, a PET scan can produce images of cancerous tumors which doctor can suggest what treatment is preminent. Cancerous tissue, which uses more glucose than customary body tissue, will turn up as a vivid area on the PET image. Three-dimensional images of tracer concentration within the body are then constructed by computer analysis. Positron Emission Tomography (PET) has become an essential diagnostic tool for physicians to reveal the presence and severity of cancers. PET image helps to determine whether the therapy is working or not and detect any recurrent tumors.

This paper presents the reconstruction of PET brain image using weighted least-squares (WLS) [5]. It is a statistical method based on the iteration approach. It provides better result compared to analytical approach. A PET scan can indicate whether the tumor will respond to the treatment or not for brain cancer. Brain cancer is such a deadly disease because it can grow for many years before it is diagnosed and often spreads before it is found. Brain tumors may also spread from cancers primarily located in other organs. Brain tumor is inherently serious and life-threatening because of its invasive and infiltrative character in the limited space of the intracranial cavity.

II. Image Reconstruction

The reconstruction of PET data's are measured by the tomography is achieved by a computer system. The main intention of PET image reconstruction is to epitomize the internal structure of a subject, based on the detection of the radiation emitted by the body after introducing a radiopharmaceutical [2], [3]. This process takes place in 2D or 3D acquisition modes and 2D or 3D reconstruction algorithms can also be employed. Different kinds of reconstruction algorithms can be used (analytical or iterative) depending on several issues such as the desired peak signal-to-noise ratio, mean square error, normalized root mean square error, etc., There are two main approaches to the image reconstructions are 1. Analytical method 2. Iteration method. There are some

routines for the reconstruction that differs in the quality of the resulting pictures and the computation time. The iterative method generates the most realistic pictures in medical applications [11-13].

III. Iteration method

The Iteration method is the most preferred method for image reconstruction. This method uses the mathematics of computed tomography related to the coincidence data in each detected tube with the activity distribution in the image, based on statistical tenets. The advantages are better noise profile and resistance to the streak artifacts common with analytical tactic because they observe the noise structure and realistic model of the system [7-10]. These improvements come at the cost of added intricacy resulting in mathematical problems without a direct analytic solution or with an analytic solution that cannot be solved with current processing potentially. Resultantly, the more pragmatic approaches are often solved with methods that sequentially perk up, or frequent, guesstimate of the unknown image. This recursive process results same as more accurate estimate than analytical reconstruction schemes, at the rate of better computational stipulates. Progresses in computation hustle and faster algorithms have helped to triumph over the computational burden of iterative methods allowing them to receive growing clinical acceptance.

A. Map Based Reconstruction

ML-EM reconstruction of PET images is habitually unhinged, and the resulting images usually carnival large variances. Exploiting over the subsequent probability rather than over the likelihood function has a regularizing effect on this hesitation [19-22].

MAP algorithm is based on the Bayesian slant. This algorithm has some problem to reconstruct the PET image but it improves the degraded image. It provides better performance compared to analytical approach [16]. According to Bayesian methodology, the posterior prospect of renovating an image is given by posterior solidity function of unobservable data x and the observed counts n [18].

$$P(\text{image} | \text{data}) = \int P(\text{image} | x, n) P(x | n) dx \quad (1)$$

$$L = \arg \max[\ln\{P(l | n)\} = \ln\{P(n | l)\} - \ln\{P(l)\}] \quad (2)$$

Most widely used utility is Gibbs distribution [10] to find out prior evidence about the neighbourhood pixels. It fines a prearranged pixel constructed on variances between the neighbouring pixels and articulated by

$$P(\lambda) = e^{-U(\lambda)} / X \quad (3)$$

X =normalization constant;

$U(\lambda)$ =energy gathering and contain aptitudes. The higher is the energy of the structure; the lower will be the prospect.

The Markov Haphazard Field model for a class of images can be modified by a Gibbs distribution like the prior probability of the activity concentration expressed by:

$$P(\lambda) = \frac{1}{X} e^{-\alpha U(\lambda)} \quad (4)$$

α is the hyper constraint that influences the degree of smoothness of the estimated images. Design of the potential function allows penalization of renovated images to smoothing or preserving edges.

$$U(\lambda) = \frac{1}{2} \sum_{i=1}^K \sum_{k \in K_m} \psi(v_i - v_j) \quad (5)$$

This algorithm is also one of the expectation maximization methodologies. This is shadowed by

$$c_i^{k+1} = \frac{c_i^k}{\sum_i C_{ij} + \alpha \frac{\partial}{\partial \lambda_k} \sum_B U_B(\lambda^{(k)})} \sum_j \frac{x_i C_{ij}}{\sum_k P_{im} \lambda_i^{(k)}} \quad (6)$$

C_{ij} is the system matrix of PET image, It represents the likelihood that an event occurred at pixel (i) in the detector (j).

B. Conjugate gradients (CG):

This sector reviews the rationale by means of the conjugate gradients (CG) algorithm for quadratic objective functions such as WLS. The WLS estimate x_{wls}^* is the key.

To the quadratic crisis with maximize equality constraints

$$S_m(y) = -\frac{1}{2} \sum_{i=0}^p \left(\frac{y_i - m_i}{\sqrt{m_i}} \right)^2 \quad (7)$$

Subject to $Ax = Y$

The pitch of the WLS purpose with respect to x is given by

$$r_n = \nabla_x S_m(y_n) \quad (8)$$

$$r_n = A^T M^{-1} (m - y_n) \quad (9)$$

Where $y_n = Ax_n$ and $M = \text{diag}(m)$

CG is the iterative scheme of choice to optimize a quadratic objective. This descent method alternates the computation of a search direction and a step size; producing a sequence of estimates x_n . The CG search direction d_n combines the gradient of the objective function S_m and the previous search direction.

$$q_n = r_n + \beta_n q_{n-1} \quad (10)$$

Where d_n defines the relative weight of each term. Several formulations exist for β_n .

In CG, the image update is performed additively as in a line search determines the step size α_n . After the line search procedure, the gradient g_{n+1} is orthogonal to the search direction d_n .

$$q_n^T r_{n+1} = 0 \quad (11)$$

The image left behind is defined as the difference between the current image estimate and the optimal WLS solution

$$e_{n+1} = x_{n+1} - x_{wls}^* \quad (12)$$

The optimal solution x_{wls}^* is satisfies $\nabla_x S_m(Ax_{wls}^*) = 0$

Using this property, the gradient can be expressed as a linear function of the residual

$$r_n = -A^T M^{-1} A e_n \quad (13)$$

The look for direction and the image left behind satisfy a conjugation relationship

$$q_n^T C e_{n+1} = 0 \quad (14)$$

Where $C = A^T M^{-1} A$ is the conjugation matrix. Following the residual e_{n+1} can be reformulated as

$$e_{n+1} = e^{i+1} + \sum_{j=i+1}^n \alpha_j d_j \quad (15)$$

For $i < n$. As a result,

$$q_n^T C e_{n+1} = \sum_{j=i+1}^n \alpha_j d_i^T C d_j \quad (16)$$

The solution to WLS-CG is to use Gram-Schmidt orthogonalization procedure to construct a basis of conjugate search directions (d_i) that satisfy

$$q_i^T C d_j = 0, i \neq j$$

For such a basis of conjugate directions, implies that the residual is conjugate to all the past search directions

$$e_n^T C d_i = 0, i < n$$

In other words, $n-1$ components of e_n are zero in the C-orthogonal basis defined by (d_i). As n increases, the image residuals are constrained to a subspace of decreasing dimension. In other words, the n th update does not undo the work achieved during the earlier steps. The accurate value of the outstanding is never known during the optimization, yet after $(N+1)$ iterations it is exactly zero (at least in theory). Moreover, it has been observed that small residuals can be obtained even after a number of iterations much smaller than N . Convergence is particularly fast when the eigen values of the conjugation matrix C are clustered.

For WLS-CG, conjugate search directions can be interpreted as being orthogonal when projected and normalized by the measured standard deviation of each sinogram be in

$$(M^{-1/2} A d_i) \perp (M^{-1/2} A d_j) \quad (17)$$

The Polak-Ribiere formulation builds recursively such a basis of conjugate search directions. The new search direction d^n is chosen in the subspace spanned by the gradient g^n and all the past search directions

$$q_n = r_n + \sum_{j=1}^{n-1} \beta_{n,j} d_j \quad (18)$$

The co-efficient must be such that d^n satisfies, which yields

$$r_n C d_i + \beta_{n,i} d_i^T C d_i = 0 \quad (19)$$

for $i < n$. The $n-1$ equations are uncoupled and can be solved independently, which yields the Polak-Ribiere formulation.

C. *Pollak ribeire -cg method:*

Pollak-Ribeire form of the CG method is:

$$p^k = \nabla \varphi(f^k) \quad (20)$$

$$\beta^K = \frac{(\nabla \varphi(f^K) - \nabla \varphi(f^{K-1}))^T \varphi^K}{(\nabla \varphi(f^{K-1}))^T p^{K-1}} \quad (21)$$

$$\alpha^k = p^k + \beta^k d^{k-1} \quad (22)$$

$$\alpha^k = \arg \text{Max} \varphi(f^k + \alpha d^k) \quad (23)$$

$$f^k = f^{k+1} + \alpha^k d^k \quad (24)$$

CG methods accelerate the steepest descent method by choosing mutually conjugate search directions. In the above set of equations, d^k denotes the search direction and α^k is the step size determined by performing a 1-D optimization along d^k [14,22]. For non-quadratic problems, we need to perform a line search to determine α^k , but for our quadratic problem, a closed form solution is existing. Conjugate gradients frequently work well in common problems and require no enormous matrix inverses.

D. ARTIFICIAL NEURAL NETWORK

Review Stage

In this paper used a three layer BPNN method reconstruction. The image is used for reconstruction, it is divided into blocks and taken to input neurons, the reconstructed image is taken from the output of the hidden layer .there are three layer input, hidden and output. The output of the network is equal to the input pattern with each layer in a narrow channel. The normalized gray level range, training sample of block are converted into vectors [15, 16, 17]. The output of neuron can be written as

$$S^l = e_p + n^l \quad (25)$$

Where n is the bias vector. In ANN, sonogram is treated as a neural output, and p is also neural input. e is the weight matrix between the neuron input and output.

TRAINING ALGORITHM

1) The input and the output with maximum values (i.e.) when the input and output lie between 0 & 1 better output will be obtained.

2) Initialize the weights connecting the input neurons and hidden neurons, such that value between 0 and 1.

3) Compute the output of input layer then compute the input to the hidden layer.

4) Find the error (difference between the network output and the desired output).

5) Find the weight adjustments until the error reach the

desired level.

Train the neural network with the 1089 X×Y×Z data block. The X×Y is the input of the network, and the Z is the training objective. Train the network 500 times. In the process of each time, it has to input 1089 coordinate value X×Y and the target color-level value Z [5]. Then, the neural network stores the information of the map through its individual composition. In genus to export the data block to the Mat lab Neural Network Tool (NNTOOL) as the teaching sample, it need to convey the coordinate matrix X, Y into a matrix which include 2 row and 1089 arrange.

IV. Evaluation parameters

Image quality measures are figures of merit used for the evaluation of imaging systems [6]. It shows the efficiency of the algorithm and indicates the result. The efficiency of the reconstruction algorithm is generally measured using image quality criteria. A good image quality measure should well reflect the distortion on the picture due to blurring, noise, compression, sensor meagreness. In the image coding and mainframe idea literature, the most recurrently used measures are deviations between the innovative and the coded images with Peak Signal to Noise Ratio (PSNR) diversities being the most common measures. The reasons for their widespread attractiveness are their mathematical tractability and the fact that it is often straightforward to design systems that minimize the MSE.

The PSNR is used to evaluate image quality. These measures are calculated from a set of images generated from the same source and passed through the same reconstruction process. The PSNR is defined as the ratio between the original image and the power of distorting noise that affects the quality of its representation. And the mean square error is defined as the ratio between cumulative squared error between the reconstructed and the original image.

The PSNR will be calculated by the following equation,

$$PSNR = 20 \log \frac{MaxN}{\sqrt{MSE}} \quad (26)$$

The NRMSE expresses a normalized measure of agreement between the reconstructed image $y(i, j)$ and actual image $x(i, j)$. The RMSE and NRMSE will be calculated by the following equation,

$$NRMSE = \sqrt{\frac{\sum_{i=0}^{m-1} \sum_{j=0}^{n-1} (y(i, j) - x(i, j))^2}{\sum_{i=0}^{m-1} \sum_{j=0}^{n-1} (x(i, j))^2}} \quad (27)$$

$$NAE = \frac{1}{K} \sum_{k=1}^K \frac{\sum_{i,j=0}^{n-1} y(i, j) * \bar{y}(i, j)}{\sum_{i,j=0}^{N-1} y(i, j)^2} \quad (28)$$

$$AD = \frac{1}{MN} \sum_{i=0}^{M-1} \sum_{j=0}^{N-1} \{y(i, j) - \bar{y}(i, j)\} \quad (29)$$

The average difference is also used to measure the error in the images. These all evaluation measures are not only needed for comparing images produced by dissimilar techniques, but it is as well instrumental in designing image reconstruction algorithms.

V. Simulation and Results

The simulations were achieved using MATLAB-Simulink and verified using mathematical equations. We have chosen brain image in 3 dimensions for scrutiny. In recursive reconstruction algorithm, we have to predefine some parameters for comparing their results with previous iteration algorithm. Various image quality parameters are also calculated from the analysis. Figure 1, 3 and 6 shows the simulation results for iteration 5,20,30,40 and 50 using MAP, CG and NNCG algorithm respectively.

Image quality loss occurred from artefacts depends on environment and components in scanner of the artefacts as well as the context or background in which they occur. Many parameters are used here for analyzing the image quality such as NRMSD,PSNR,AD and NAE.

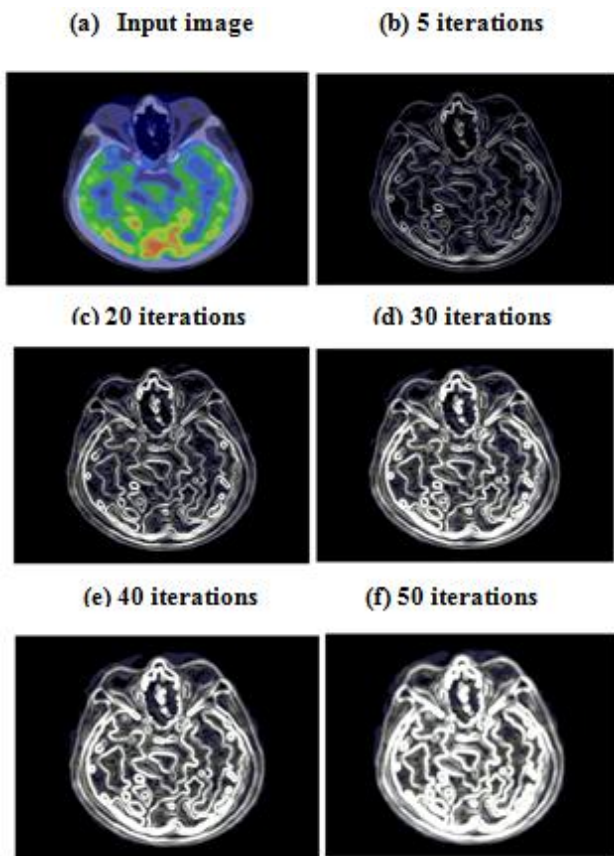


Figure 1 shows the simulation results for MAP Algorithm (a) Input image, (b) after 5 iterations, (c) after 20 iterations, (d) after 30 iterations, (e) after 40 iterations, (f) after 50 iterations

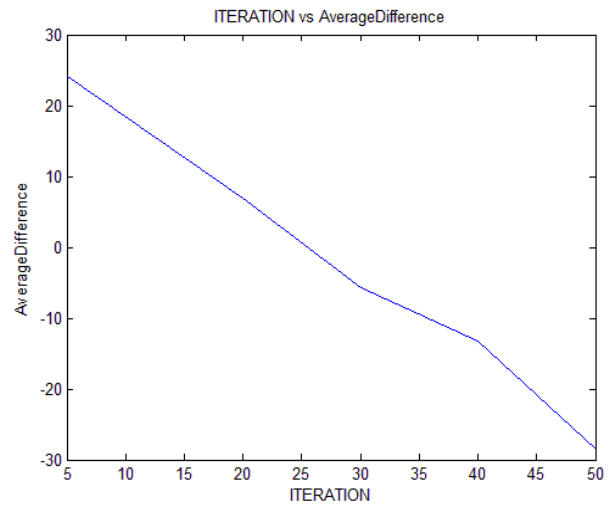


Fig. 2.a

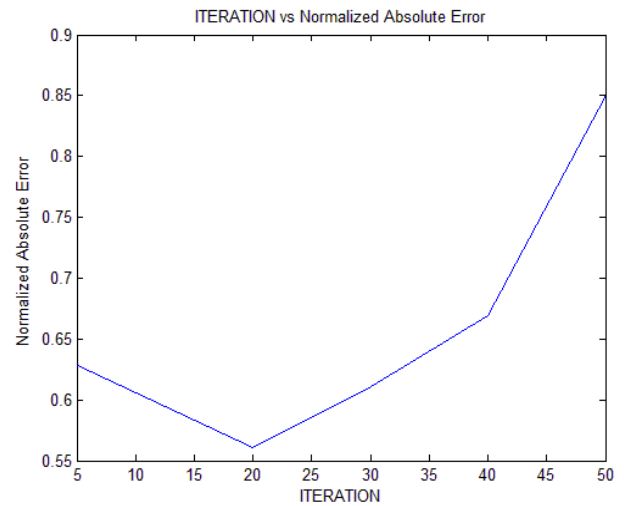


Fig. 2.b

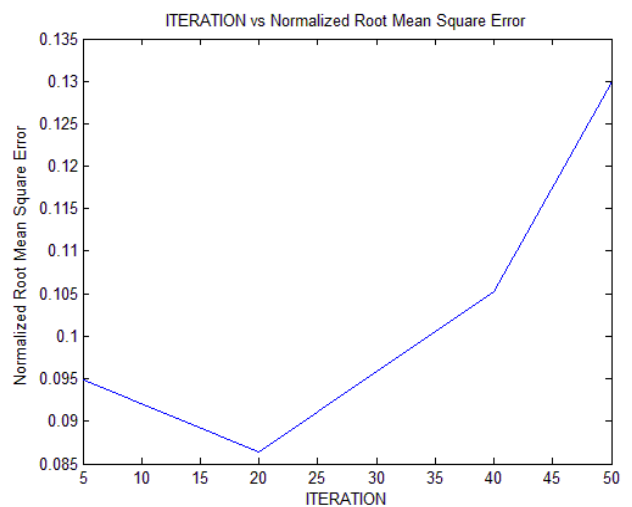


Fig. 2.c

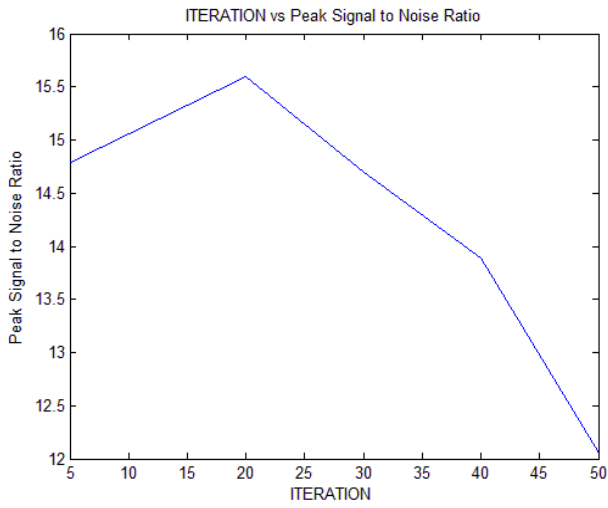


Fig. 2.d

Figure 2 shows the graph for image quality measures using MAP. (a) Iteration vs. Average Difference (b) Iteration vs. Normalized Absolute Error (c) Iteration vs. Normalized Root Mean Square Deviation (d) Iteration vs. Peak Signal to Noise Ratio

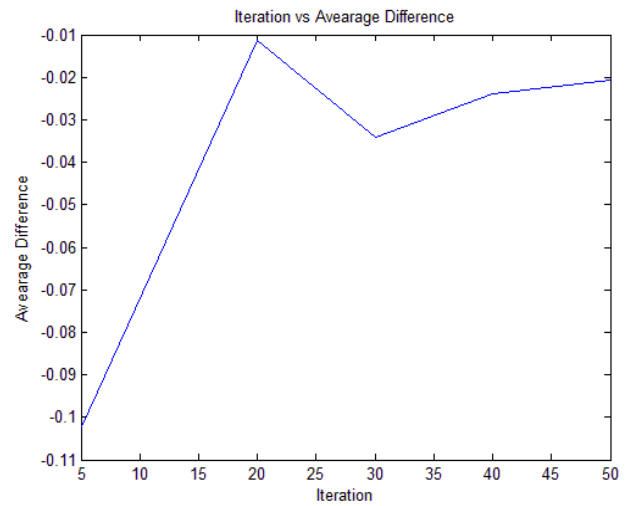


Fig. 4.a

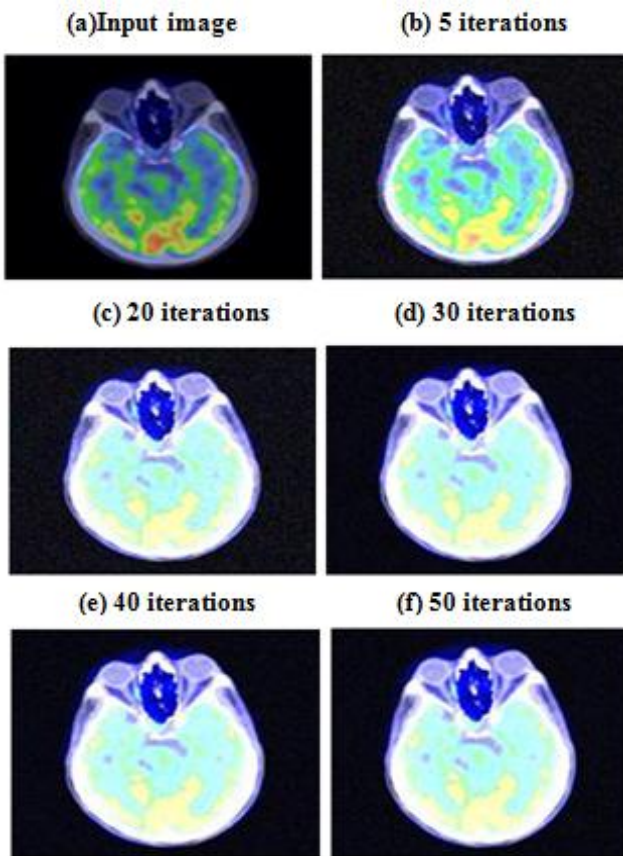


Figure 3 shows the simulation results for CG Algorithm (a) Input image, (b) after 5 iterations, (c) after 20 iterations, (d) after 30 iterations, (e) after 40 iterations, (f) after 50 iterations

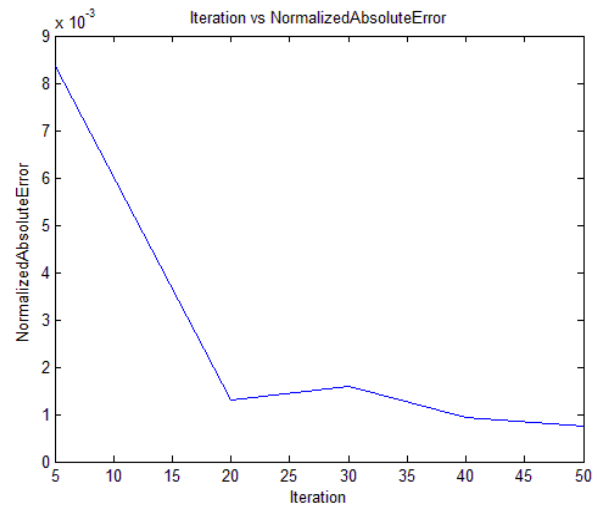


Fig. 4.b

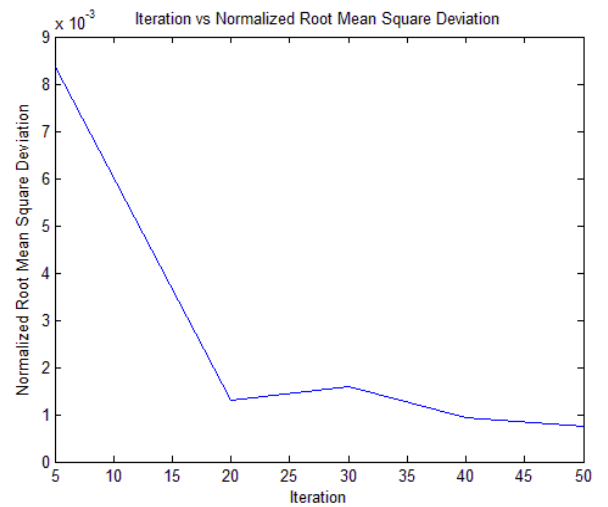


Fig. 4.c

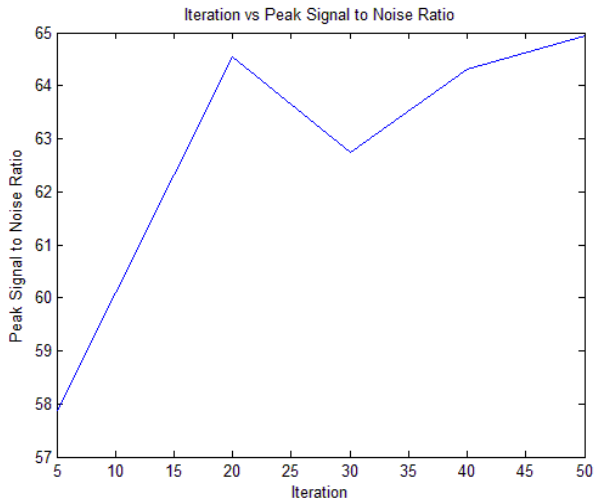


Fig. 4.d

Figure 4 Shows the graph for image quality measures using MAP. (a) Iteration vs. Average Difference (b) Iteration vs. Normalized Absolute Error (c) Iteration vs. Normalized Root Mean Square Deviation (d) Iteration vs. Peak Signal to Noise Ratio

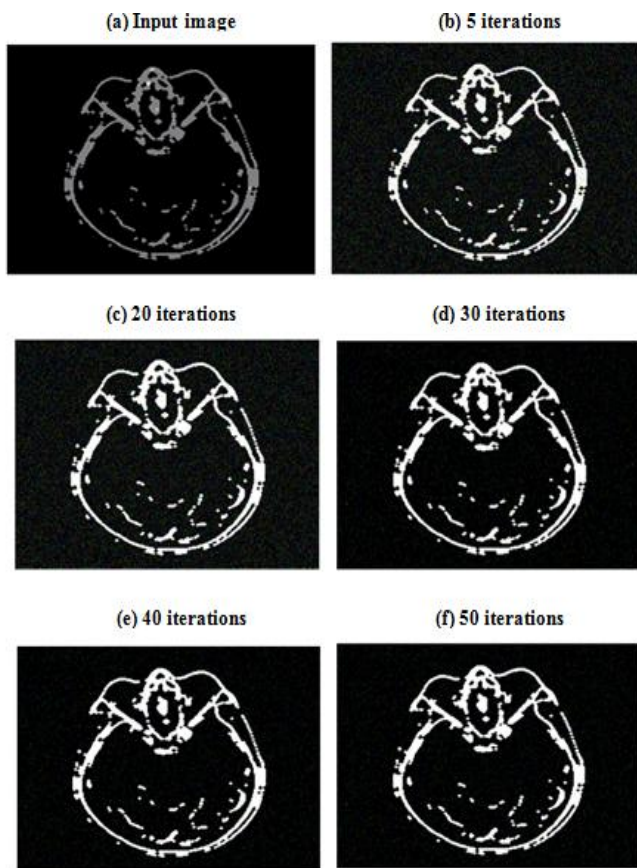


Figure 5 shows the simulation result for NNCG algorithm. (a) Input PET Brain Image (b) after 5 iterations, (c) after 20 iterations, (d) after 30 iterations, (e) after 40 iterations, (f) after 50 iterations

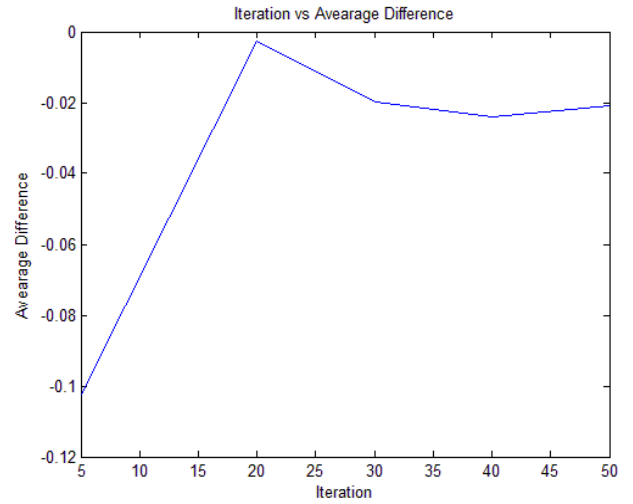


Fig. 6.a

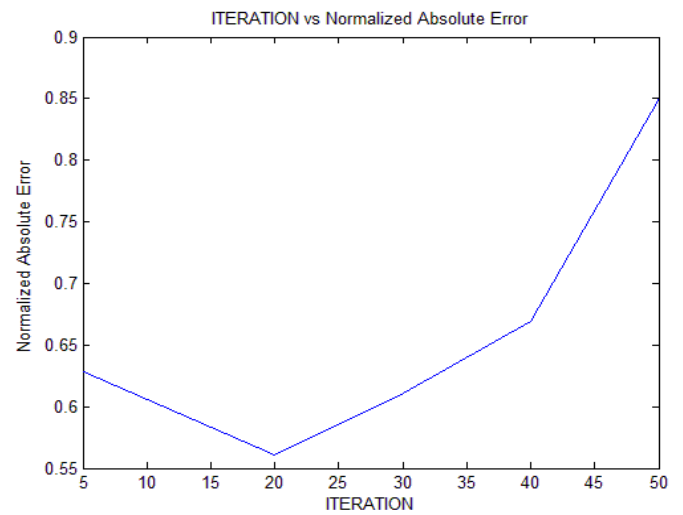


Fig. 6.b

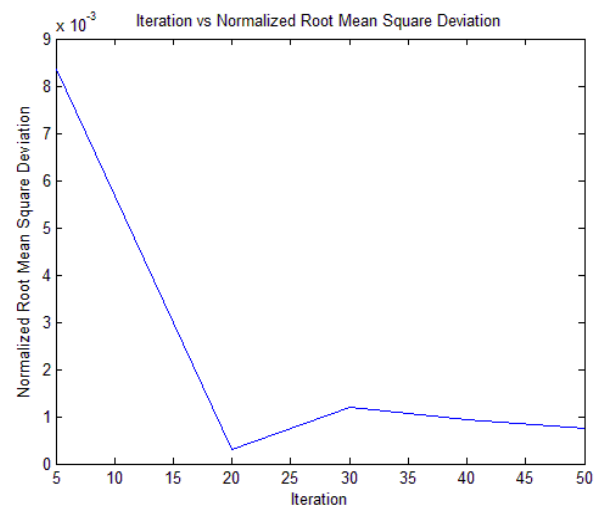


Fig. 6.c

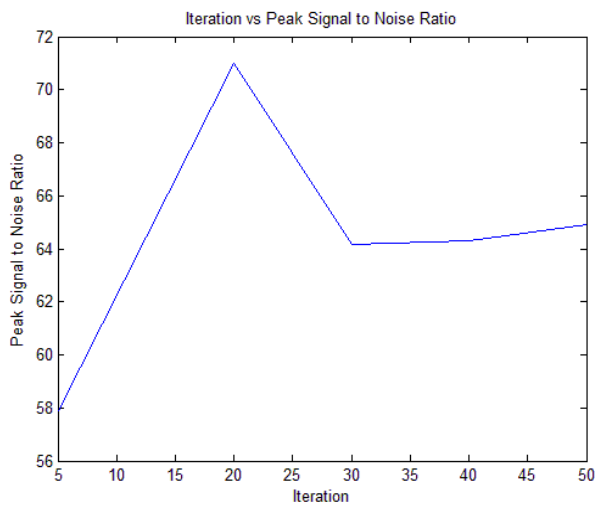


Fig.6.d

Figure 6 shows the graph for image quality measures using MAP. (a) Iteration vs. Average Difference (b) Iteration vs. Normalized Absolute Error (c) Iteration vs. Normalized Root Mean Square Deviation (d) Iteration vs. Peak Signal to Noise Ratio

TABLE I

VALUES FOR VARIOUS ITERATION RESULT

Iteration	AD		
	MAP	CG	NNCG
5	24.0831	-0.1021	-0.1021
20	6.9034	-0.0114	-0.0026
30	-5.6333	-0.0341	-0.0199
40	-13.2552	-0.0239	-0.0239
50	-28.5281	-0.0207	-0.0207

TABLE II

VALUES FOR VARIOUS ITERATION RESULT

Iteration	NAE		
	MAP	CG	NNCG
5	0.6281	0.1021	0.1021
20	0.5609	0.0649	0.0649
30	0.6113	0.0341	0.0366
40	0.6689	0.0239	0.0239
50	0.8499	0.0207	0.0207

Table I and Table II shows the calculated image quality parameters value for various iteration of MAP, CG and NNCG algorithm. Average Difference (AD), Normalized Absolute Error (NAE).

TABLE III

VALUES FOR VARIOUS ITERATION RESULT

Iteration	NRMSD		
	MAP	CG	NNCG
5	0.0948	0.0084	0.0084
20	0.0864	0.0013	2.9423E-004
30	0.0959	0.0016	0.0012
40	0.1052	0.00092819	9.2819E-004
50	0.1300	0.00074487	7.4487E-004

TABLE IV

VALUES FOR VARIOUS ITERATION RESULT

Iteration	PSNR		
	MAP	CG	NNCG
5	14.7922	57.8719	57.8719
20	15.6006	64.5527	70.9756
30	14.6932	62.7418	64.1687
40	13.8900	64.3065	64.3065
50	12.0493	64.9344	64.9344

Table III and Table IV shows the calculated image quality parameters value for various iteration of MAP, CG and NNCG algorithm. Peak Signal to Noise Ratio (PSNR), Normalized Root Mean Square Deviation (NRMSD).

Conclusion

Thus PET is an exciting nuclear medicine technique that facilitates the evaluation of the chemical and physiological changes associated with the metabolic processes in the human body via the use of non-invasive diagnostic imaging procedures. Image reconstruction for PET using iterative algorithms provides more accurate modeling of the PET data (in terms of the acquisition process and the statistical noise). This paper deals with MAP and CG algorithm. The most frequently used method such as CG, each iteration update the image and compare with previous iteration. To better up the results of CG, Neural Network was implemented in CG algorithm in image segmentation, to maximize the likelihood function of the renovated image. It is concluded that Neural Network based CG algorithm have better image reconstruction quality.

Acknowledgment

We thank Anderson Diagnostics and Lab, Chennai for providing the Liver PET images for our research and Department of Instrumentation and Control Engineering of Kalasalingam University, (Kalasalingam Academy of Research and Education), Tamil Nadu, India for permitting to use the computational facilities available in biomedical Laboratory which was setup with the support of the Department of Science and Technology (DST), New Delhi under FIST Program.

References

- [1] G. H. Golub and C. F. Van Loan, *Matrix Computations*, Second Edition. Baltimore, MD: The Johns Hopkins University Press, 1989.
- [2] T. F. Budinger, G. T. Gullberg, and R. H. Huesman, "Emission computed tomography," in *Image Reconstruction from Projections: Implementation and Applications*.
- [3] G. T. Herman, *Image Reconstruction from Projections: The Fundamentals of Computerized Tomography*. New York: Academic Press, 1980.
- [4] M. M. Ter-Pogossian, M. Raichle, and B. E. Sobel, "Positron emission tomography," *Sci. Amer.*, vol. 243, no. 4, pp. 170-181, 1980.
- [5] R. H. Huesman, G. T. Gullberg, W. L. Greeberg, and T. F. Budinger, "User manual, *Donner algorithms for reconstruction tomography*," Lawrence Berkeley Lab., Univ, California, 1977.
- [6] Sarita Kumari and Ritu Vijay, "Image Quality Estimation by Entropy and Redundancy Calculation for Various Wavelet Families", *International journal of computer information systems and industrial management applications*, pp. 27-34, Vol.4, 2012.
- [7] Z. Liang, D. Gilland, R. Jaszczak and R. Coleman, "Implementation of Non-Linear Filters for Iterative Penalized Maximum Likelihood Image Reconstruction", *IEEE* 1990.
- [8] E. Karali, S. Pavlopoulos, S. Lambropoulou, and D. Koutsouris, "ISWLS: Novel Algorithm for Image Reconstruction in PET," *IEEE trans on information technology in biomedicine*, vol. 15, no. 3, May 2011.
- [9] V.K. Madan, "PET Instrumentation and Image Reconstruction," in *Seminar on Positron Emission Tomography: Technology and Application*, Krishnankoil, July 30, 2011.
- [10] Sanghee Cho, Quanzheng Li, Sangtae Ahn, Bing Bai, and Richard M. Leahy, "Iterative Image Reconstruction Using Inverse Fourier Rebinning for Fully 3-D PET", *IEEE Trans. ON Med. Imag.*, vol. 26, no. 5, May 2007.
- [11] Guobao Wang, Jinyi Qi, "Iterative nonlinear least squares algorithms for direct reconstruction of parametric images from dynamic pet," *IEEE Trans. Med. Imag.*, vol. 18, no. 5, pp. 393-403, 2008.
- [12] Brent A. Williams and David G. Long, "Reconstruction From Aperture-Filtered Samples With Application to Scatterometer Image Reconstruction", *IEEE Trans. on Geoscience and Remote Sensing*, Vol 49, No. 5, May 2011.
- [13] P. Khurd, Y. Xing, I. T. Hsiao, and G. Gindi, "Fast Preconditioned Conjugate Gradient Reconstruction for 2D SPECT", in *Conf. Rec. IEEE Nuc. Sci. Sym. Med. Imaging Conf.*, San Diego, 2002, pp. 741-745 vol.2, IEEE.
- [14] Karras, D.A., Reczko, M., Mertzios, V., Graveron-Demilly, D, van Ormondt, D., Papademetriou, R.C., "Neural network reconstruction of MR images from noisy and sparse k-space samples", *International Conference on Signal Processing*, 2000.
- [15] Singh G, Khasnobish, A, Jati, A, Bhattacharyya, S, Konar, A, Tibarewala, D.N, Janarthanan R, "Object-shape classification and reconstruction from tactile images using image gradient", *International Conference on Emerging Applications of Information Technology (EAIT)*, 2012.
- [16] T. Arunprasath, M. Pallikonda Rajasekaran, S. Kannan, R. Bala Murali Pandian, "Image Renovation in Positron Emission Tomography Using Recursive Algorithm", *International Conference on Computational Intelligence and Computing Research (ICCIC 2012)*, Coimbatore, India, December 18-20, 2012.
- [17] Jianwei Li, Xiaoguang Yang, Youhua Wang, Ruzheng Pan, "An Image Reconstruction Algorithm Based on RBF Neural Network for Electrical Capacitance Tomography", *International Conference on Electromagnetic Field Problems and Applications (ICEF)*, 2012.
- [18] Ok Kyun Lee, Hua Li, Sung Ho Tak, Jong Chul Ye, "Compressed sensing reconstruction of statistical parameter map for functional diffuse optical tomography", *IEEE International Symposium on Biomedical Imaging (ISBI)*, 2012.
- [19] Kamencay. P, Breznán. M, Jelsovka. D, Zachariasova. M, "Sparse disparity map computation from stereo-view images using segment based algorithm", *International Conference on Radioelektronika*, 2012.
- [20] Vunckx, K, Atre. A, Baete. K, Reilhac. A, Deroose. C.M, Van Laere. K, Nuyts. J, "Evaluation of Three MRI-Based Anatomical Priors for Quantitative PET Brain Imaging", *IEEE Trans. On Medical Imaging*, 2012.
- [21] Yong Xia, Lingfeng Wen, Eberl. S, Fulham. M, Dagan Feng, "Segmentation of dual modality brain PET/CT images using the MAP-MRF model", *IEEE Workshop on Multimedia Signal Processing*, 2008.
- [22] T. Arunprasath, M. Pallikonda Rajasekaran, S. Kannan, V. Adithiyaa, "Reconstruction of PET Brain Image using Conjugate Gradient Algorithm", *Second World Congress on Information and Communication Technologies (WICT 2012)*, Trivandrum, India, October 30-31, November 1-2, 2012.
- [23] V.E. Asadchikov, A.I. Chulichkov, A.V. Buzmakov, M.V. Chukalina, D.P. Nikolaev, R.A. Senin and G. Schaefer, "Morphological Analysis and Reconstruction for Computed Tomography", *International journal of computer information systems and industrial management applications*, pp. 27-34, Vol.3, 2011.

Author Biographies



First Author T. Arun prasath was born at kumbakonam, India in 1985. He graduated in Electrical and Electronics Engineering from Anna University and post graduated in Applied electronics in 2009 from Anna University of technology, Trichirapalli, India. He is doing Ph.D (Non Linear PET Image reconstruction) in Kalasalingam University, Krishnankoil. Now he is working as Assistant Professor in the Department of Electrical and Electronics Engineering, Kalasalingam University. He has published 6 papers in international level Conferences and 5 National level Conferences. His research interests include Digital image processing, Network processor and Bio-medical Instrumentation.



Second Author M. Pallikonda Rajasekaran was born at Bodinayakanur, India in 1980. He graduated in Electronics and Instrumentation Engineering from Bharathidasan University and post graduated in Biomedical Signal Processing and Instrumentation from SASTRA University in the year 2001 and 2002 respectively. He received his Ph.D (Remote Patient Monitoring System Using Wireless Sensor Networks) in 2009 from Anna University, Chennai, India. Now, he is working as Professor in the Department of Instrumentation and Control Engineering, Kalasalingam University. He has published 7 papers in international Journals and 25 papers in International Conferences. His research interests include Telemedicine, Wireless Sensor Networks, Healthcare, Embedded Systems and Signal Processing.



Third Author S. Kannan received B.E, M.E, and PhD Degrees from Madurai Kamaraj University, India in 1991, 1998 and 2005 respectively. He is Professor and Head of Electrical and Electronics Engineering, Kalasalingam University, Krishnankoil-626190, India, where he has been since July 2000.